Experimental Studies on the Evolvement of Electrical Resistivity during Methane Hydrate Formation in Sediments

ARTICLE *in* ENERGY & FUELS · SEPTEMBER 2012

Impact Factor: 2.79 · DOI: 10.1021/ef301257z

9 AUTHORS, INCLUDING:

Chang-Yu Sun
China University of Petroleum
107 PUBLICATIONS **1,279** CITATIONS
SEE PROFILE

Shengli li
Jilin University
7 PUBLICATIONS **15** CITATIONS
SEE PROFILE

X.q. Guo
China University of Petroleum
25 PUBLICATIONS **408** CITATIONS
SEE PROFILE

energy&fuels

Article

pubs.acs.org/EF

Experimental Studies on the Evolvement of Electrical Resistivity during Methane Hydrate Formation in Sediments

Feng-Guang Li,[†,‡] Chang-Yu Sun,[*,†] Sheng-Li Li,[†] Guang-Jin Chen,[*,†] Xu-Qiang Guo,[†] Lan-Ying Yang,[†] Heng Pan,[†] Shi Li,[‡] and Ke Zhang[‡]

[†]State Key Laboratory of Heavy Oil Processing, China University of Petroleum, Beijing 102249, China

[‡]Research Institute of Petroleum Exploration and Development, PetroChina, Beijing 100083, China

ABSTRACT: An experimental setup was developed to in situ measure the evolvement of the electrical resistivity during hydrate formation process to aid the interpretation of the influence of hydrate saturation on the electrical properties of the sediment. Five hydrate samples under different initial brine saturations of 12, 20, 30, 40, and 50% were formed from free methane gas and brine with 3.35 wt % NaCl in the 60−80 mesh sandy sediment, during which the variations of electrical resistivity were in situ measured. It was observed that the resistivity of the hydrate-bearing sediment increases with the increase of hydrate saturation during the hydrate formation process and finally achieves a constant value for each group of hydrate sample. For hydrate samples at different initial brine saturations, the values of electrical resistivity are larger, even though hydrate saturation is lower if free methane gas exists in sediment pores. Based on the measured electrical resistivity of hydrate-bearing sediment before and after brine injection at different hydrate saturations, parameters in Archie equation were determined to describe the relationship between resistivity and hydrate saturation, which would be helpful for mapping the hydrate concentration in the sediment through resistivity logging data from hydrate deposits.

1. INTRODUCTION

Clathrate hydrates are nonstoichiometric, crystalline compounds that form from light hydrocarbon gas molecules and water at relatively low temperature and high pressure conditions.[1] Natural gas hydrates are widely discovered in the shallow ocean bottom and permafrost regions, and the main component is methane gas. The global volume of gas hydrate is enormous, and a significant portion of the total volume is expected to be technical recoverable.[2] Research interest in natural gas hydrate increases as the abundant applications of hydrates in solving energy and environment problems.[3−5] It is of first importance to map natural gas hydrate distributions before its exploitation. Some remote sensing techniques are therefore needed, which rely on detecting the variation of signal arisen from the sediment.

Electrical resistivity measurement from well logs and from controlled-source electromagnetic methods has been used for gas hydrate identification and quantification.[2−12] To better associate electrical properties measured in the field with specific gas hydrate concentration and distribution patterns, it is important to examine the relationship between the electrical resistivity data with the properties of lab-created hydrate-bearing sediment.[2] Some laboratory research has been performed in the literature. For CO_2 hydrate in the sediment, Buffett and Zatsepina[13,14] found that the resistance increases with the increase of hydrate concentration during the hydrate formation process. Pearson et al.[15] tested electrical resistivity of hydrate formed from tetrahydrofuran solution with the Berea Sandstone and Austin Chalk samples at atmospheric pressure and suggested that the electrical resistivity increases along with the hydrate formation and it was strongly a function of the dissolved salt content of the pore water. Lee et al.[16] also conducted laboratory experiment to form tetrahydrofuran hydrate and pointed out that both permittivity and electrical conductivity (or resistivity) are good indicators of the volume fraction of free water in the sediment, which is, in turn, dependent on hydrate saturation. Li et al.[17] and Ren et al.[18] measured the electrical resistance of a large sandpacks simulating the conditions of hydrate formation in subsea sediments. The results showed that resistivity increases with the increase of hydrate concentration to a great extent and finally achieves a constant value of 11−13 Ω·m after the completion of hydrate formation process.

It is known that electrical resistivity is dependent on aqueous solution, fluid-filling porosity, ionic concentration of the pore fluid, and other conduction effects. The presence of gas hydrate and its distribution have great effects on the measured results of electrical resistivity of hydrate-bearing sediment.[4,6,9,10] The estimation of the hydrate content using downhole electrical measurements based on Archie's law requires the knowledge of the saturation exponent. However, there are a lot of influencing factors that would affect the value of saturation exponent, such as lithology, the intergranular pore space, and the distribution of the brine in the sediments. Though some researchers[3,7,19] have done some work about the relationship between gas hydrate content with the electrical properties of hydrate-bearing sediment, it is far from enough for the geophysical investigation. In addition, the existing studies on electrical resistivity of hydrate are insufficient, especially for hydrate-containing sediments similar to the real stratum environment. Extensive and consistent laboratory data for the electrical resistivity of hydrate is needed to exactly interpret the electrical

Received: May 8, 2012
Revised: September 11, 2012
Published: September 28, 2012

resistivity logs field data. In this work, an experimental apparatus for synthesizing hydrate sample and measuring the variation of electrical resistivity during hydrate formation was built. The hydrate sample (a mixture of sand packs, methane hydrate, and brine) with uniform hydrate distribution under in situ conditions of permafrost regions or deep ocean seas was synthesized from brine and free methane gas within partially brine-saturated sediment to examine the exact relationship between hydrate saturation and electrical resistivity. The evolvement of electrical resistivity of hydrate-bearing sediment with the formation of hydrate was investigated. The parameters of the Archie formula were also inferred. The obtained physical properties of hydrate-bearing sediments will be valuable for the development of geophysical techniques to locate and characterize natural gas hydrate deposits.

2. EXPERIMENTAL SECTION

2.1. Experimental Apparatus. An experimental system was designed and built for synthesizing gas hydrate and measuring the variations of electrical resistivity during hydrate formation process. A schematic diagram of the experimental device is shown in Figure 1,

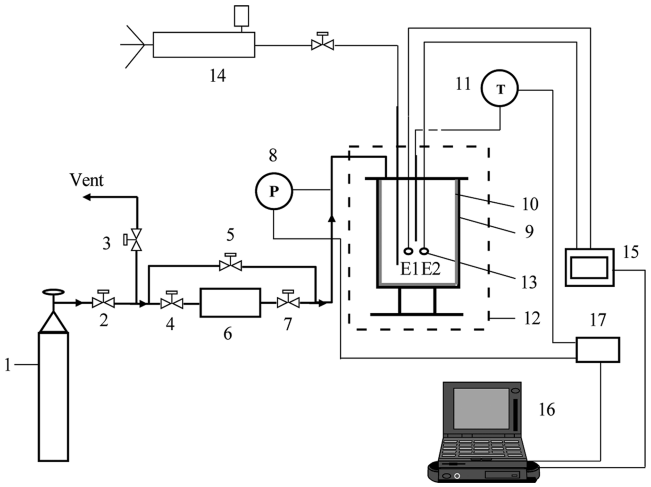

Figure 1. Schematic diagram of the experimental apparatus for measuring the electrical resistivity of hydrate-bearing porous media during hydrate formation and dissociation processes: 1, gas cylinder; 2, 3, 4, 5, 7, valve; 6, gas mass flowmeter; 8, pressure transducer; 9, reactor; 10, a PTFE tube; 11, Pt100 thermometer; 12, cold-chamber; 13, two-electrode configuration; 14, hand pump; 15, digital electric bridge; 16, personal computer; 17, data collecting modulus.

which mainly contains a high pressure reactor, an air bath, a gas flowing system, and a data collection system. The reactor is made by Jiangsu Hua'an Oil Scientific Research Apparatus Co., Ltd., China, with a volume of about 2.0 L (ϕ 130 × 150 mm) and a maximum working pressure of 30.0 MPa. A plate with an O-ring seal, in which several openings with a diameter of 3 mm are prepared to install measurement elements, is bolted to the top of the reactor. A Pt100 thermometer is inserted into the sediments through the lid of the high pressure reactor with a precision of ±0.1 K. The pressure is monitored by an absolute pressure transducer with an accuracy of 0.5% at the gas filling line. The mass of methane gas injected into the reactor during the experimental process is measured by a gas flowmeter (Model DMF-1-1, made by Beijing Sincerity Automatic Equipment Co., Ltd.) with a precision of 0.1%, and its working pressure range is 0−25 MPa. A two-electrode configuration is fixed in parallel in polyterafluoroethylene (PTFE) materials due to its superiorities of high chemical stability, insulation, and unlikelyhood of metamorphosis. The electrical resistivity is measured by a digital electrical bridge through the two-electrode configuration placed in the sandy sediment. The schematic diagram of the measurement system in random packing grains is shown in Figure 2. The electrode is made by stainless steel with a

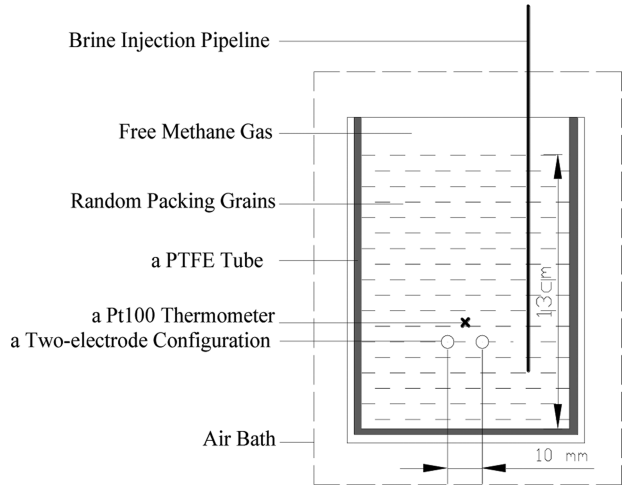

Figure 2. Schematic diagram of the measurement system in random packing grains. The whole high pressure cell is placed in the cold chamber. A two-electrode configuration that is placed horizontally in the middle of the porous sediment is used to measure electrical resistivity.

diameter of 2 mm and 58 mm in length. The two electrodes are fixed in parallel in the PTFE material. The space between the two electrodes is approximately 10 mm. During the electrical measurement, the imposed voltage is 1.0 V with a frequency of 1.0 kHz, which could minimize the effects such as electrode polarization, electrochemical reactions on electrodes, etc.

2.2. Preparation of Methane Hydrate-bearing Sample. The methane hydrate-bearing sample was synthesized by free methane gas and brine in the pore space of random packing grains under relatively high pressure and low temperature conditions. Methane gas with a purity of 99.9% was supplied by Beijing AP Beifen Gases Industry Co. Ltd. The concentration of the NaCl aqueous solution is 3.35 wt %, and the diameter of the sandy grains with a porosity of 41.68% (of the total volume) is from 300 to 200 μm (60 to 80 mesh). The sandy sediment is prepared by first washing with deionized water and then dried in the oven at 393.2 K for 24 h.

It is of importance to form hydrate similar to that of in nature because gas hydrate morphology in the sediment is a crucial factor effect on the measured result of resistivity.[2,19,20] For example, to obtain hydrate sample as that in a North Slope, one would need to create the brine and gas concentration by carefully injecting methane into 100% brine saturated sediment. In our preliminary study according to this method, we found that the hydrate could not homogenously disperse within the pore space of the sediment. Much hydrate would form on the surface of the sediment sample due to the capillary effect. Some nodule or big blocks would also exist in the sediment, which would greatly change the distribution of the brine in the sediment. This, in turn, has more influence on the measured resistivity and will result in much more of a difference from that under the natural environment. To better investigate the variation of electrical resistivity during methane hydrate formation, the sample formed with a uniform distribution is preferred in this work. To avoid the inhomogeneous hydrate distribution caused from the migration of water within the pore space of the sediment during hydrate formation due to the capillary effects,[21−24] we synthesized the hydrate sample with the following method:

First, the dried sand and brine were cooled to approximately 273.2 K. Subsequently, they were mixed quickly to disperse the brine homogeneously in the sand to prepare the fixed brine saturated sediment at a low temperature.

dx.doi.org/10.1021/ef301257z | Energy Fuels 2012, 26, 6210−6217

Second, as shown in Figure 2, a PTFE tube was put into the cell to insulate the brine solution with the inner wall of the stainless cell before the sand was loaded into the high pressure cell. Then, a two-electrode configuration was oriented horizontally in the middle of the porous sediment to investigate the change of electrical resistivity, and the partially brine saturated sediment was loaded into the PTFE tube. A Pt100 thermometer was placed above the electrodes to monitor the variation of temperature. A pipeline was inserted into the sediment at a position that was lower than the measuring electrodes through the top lid of the high pressure reactor. The layer of porous media at the base of the vessel was approximately 13 mm depth, and the two-electrode configuration was emerged in the packing grain sand completely, as shown in Figure 2. There was still a little free space at the top of vessel.

Finally, the vessel and connected pipeline were vacuumized for 20 min to eliminate the interference of air in the system, and then, free methane gas from gas cylinder was charged into the vessel up to approximately 7.5 MPa where a gas mass flowmeter was used to exactly quantify the injected methane gas amount. The temperature of the system was controlled at a relatively low value by air chamber. After gas injection, the temperature of the vessel was maintained at approximately 276.2 K to form methane gas hydrate in the sediment.

In this experiment, the temperature of partially brine-filled sand packs was well below the phase equilibrium value of methane (about 282.0 K at pressure of 7.5 MPa calculated according to Chen and Guo[25]) because the sediment and brine were precooled to 273.2 K. Therefore, the period of induction was extremely short and the hydrate nucleation process was assumed to occur simultaneously throughout the sandy sediment. Methane hydrate would then accumulate after gas injection with abundance of methane. The capillary effect was expected to be small and eliminated. To check whether the formed hydrate distributes homogeneously or not in the sediment, we synthesized hydrate-bearing sediment in a transparent sapphire vessel following the experimental method described above. The formed sample with hydrate was shown in Figure 3. It can be seen

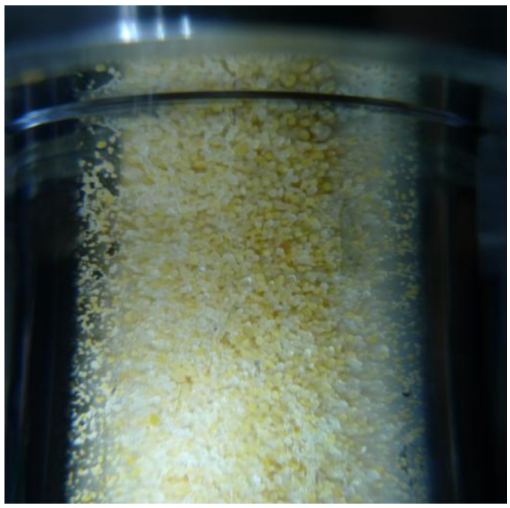

Figure 3. Formed hydrate-bearing sample in a sapphire cell.

that the formed hydrate was evenly distributed in the sand. No big hydrate blocks were found within the sand packs. The method to form a hydrate sample with uniform distribution was therefore evidently feasible.

2.3. Measurement of the Electrical Resistivity. During the hydrate formation process, the electrical resistance (R) of the hydrate-bearing sediment was in situ measured by a digital electric bridge, and the resistivity (ρ) of the hydrate sample was calculated based on the electrical resistance data. The resistance of the electrical conductor is defined as

$$R = \rho\frac{l}{A_s} \tag{1}$$

where ρ is electrical resistivity, Ω·m; l and A_s are the length and sectional area of the conductor, respectively. Here, we define K as

$$K = \frac{l}{A_s} \tag{2}$$

where K is electrode coefficient (m^{-1}), which is a constant value depending on the distance between electrodes and geometric factors of the electrode configuration and does not change during an experiment or between experiments with the same electrodes configuration. So eq 1 can be written as

$$\rho = \frac{R}{K} \tag{3}$$

If the electrical resistance of hydrate samples was measured, the resistivity can then be calculated by eq 3 according to the electric coefficient. Therefore, the value of K should be determined first. In this work, 3.35 wt % brine solution was used to calibrate the value of K. From measuring the electrical conductivity of 3.35 wt % brine solution by conductivity meter (Seven Easy F30K, made by Mettler-Toledo AG) at 276.8 K, the resistivity of the brine could be determined based on their inverse relationship. When the two-electrode configuration was placed in the brine solution, the electrical resistance could be measured by the digital electric bridge. After electrical resistivity and resistance are obtained, the electric coefficient K could then be calculated according to eq 3.

2.4. Determination of Hydrate Saturation. Hydrate saturation S_h is defined as the ratio of the total volume of formed hydrate to that of free pore space within sediment and determined by the number of moles of consumed methane gas, which was calculated from the variations of measured temperature and pressure during hydrate formation. It was used to infer the relationship between hydrate amount and the changes of electrical resistivity. Conversion ratio x is defined as the ratio of the amount of water converting to hydrate to the total amount of water in the pore space. The temperature in the porous media was assumed uniform because temperature gradients from outside to inside of the vessel were within 0.2 K among the sediment. The temperature gradient in the vessel was also neglected during hydrate formation and dissociation processes due to its effect on hydrate saturation and resistivity being extremely small. During the calculation of hydrate saturation, the volume expansion coefficient when water converts into hydrate is 1.25.[25] The detailed calculating procedure and method is similar to that proposed by Zhang et al.,[26] which was introduced as follows:

$$S_h\ (\%) = \frac{n_H n_w M_w 1.25/\rho_w}{V_{pore}} \times 100 \tag{4}$$

$$x\ (\%) = \frac{n_H n_w M_w}{m_w} \times 100 \tag{5}$$

$$n_H = n - \frac{P_{CH_4} V_{free}}{ZRT} \tag{6}$$

where n_H is the mole amount of methane consumed during hydrate formation; n_w is the hydration number, which is 5.75 for 100% cage occupancy;[26,27] M_w is the molecular weight of H_2O, 18 g/mol; ρ_w is the density of water, 1.0 g/cm^3; V_{pore} is the total pore volume of the sandy sediment; m_w is the initial mass of water (the mass of salt in the solution is subtracted); P_{CH_4} is the instantaneous pore pressure; V_{free} is the free volume, which can be calculated by the bulk volume of the reactor subtracting the volume of (sand + brine solution + hydrate); T is the instantaneous temperature of methane gas; Z is compressibility factor, which was calculated by Peng–Robinson equation of state;[28] R is the universal gas constant; n is the total mole numbers of methane injected into the vessel, which is obtained by gas flowmeter.

3. RESULTS AND DISCUSSION

3.1. Resistivity of Partially Saturated Sandy Sediment. The electrical resistivity of partially saturated sandy sediment

dx.doi.org/10.1021/ef301257z | Energy Fuels 2012, 26, 6210–6217

was first measured under 276.8 K. The measured results when at different concentrations (C_{salt}) and saturations (S_w) of brine were listed in Table 1. As shown in Table 1, for a given

Table 1. Electrical Resistivity of Partially Saturated Sandy Sediment

	resistivity, Ω·m			
S_w (%)[a]	3.35 wt % C_{salt}[b]	5 wt % C_{salt}	7 wt % C_{salt}	9 wt % C_{salt}
10	11.34	7.96	5.57	5.22
20	3.79	2.90	2.32	2.07
40	1.40	1.03	0.95	0.81
60	0.76	0.68	0.60	0.57
80	0.60	0.53	0.50	0.48
100	0.45	0.42	0.41	0.39

[a] S_w—saturation of brine in the sediment, %. [b] C_{salt} —concentration of brine.

concentration of brine, the electrical resistivity decreases sharply with the increase of brine saturation from 10% to 60%. After 60%, the variation trend tends to be slow. In addition, the resistivity of partially brine-bearing sediment decreases with the increase of concentration of NaCl (C_{salt}) in the brine. The measured resistivity data of sediment is in accordance with that of downhole electrical resistivity logs at an Ocean Drilling Program Site on the continental slope off the coast of Vancouver Island,[29] illustrating that the method proposed in this work is valid for measuring the electrical resistivity of hydrate-bearing sediment.

3.2. Variations of Resistivity during Methane Hydrate Formation. Five experimental runs were performed to examine the evolvement of in situ electrical properties during methane hydrate formation process under different initial water saturations (12, 20, 30, 40, and 50%) with salt concentration of 3.35 wt %. The exact conditions for the five runs were shown in Table 2. In this work, since the temperature gradient from the inner wall of the vessel to the internal in radial direction was only 0.2 K, its influence on electrical resistivity was extremely tiny and could be neglected. Therefore, the temperature within the sandy sediment was assumed to be uniform. The electrical resistivity (ρ_t) data before hydrate formation and after the end of hydrate formation at specified temperature, pressure, and hydrate saturation were shown in Table 2 for five samples. To aid the interpretation of the measured results, the variation of hydrate saturation S_h along with reaction time and conversion ratio of water to hydrate x were calculated according to the instantaneously temperature and pressure during hydrate formation. The variations of T, P, ρ_t, and S_h for a given initial brine saturation of 12%, 20%, 30%, 40%, and 50%, are shown in Figure 4, which were helpful to judge the hydrate formation.

As shown in Figure 4, a similar hydrate growth pattern was observed for all the five experimental runs. The experimental run with an initial brine saturation of 40% was taken as an example to interpret the variations of electrical resistivity, temperature, pressure, and hydrate saturation over the hydrate formation process. As shown in Figure 4d, before methane gas injection, the temperature of the partially saturated sediment is 275.8 K. When methane gas injection is finished, the pressure of methane gas is at 8.05 MPa and the temperature in the sand packs increases to 279.1 K, due to the latent heat by the injected methane gas at room temperature. Hydrate formation will quickly occur after gas injection with a subcooling of 3.5 K at 8.05 MPa. With the continuous formation of hydrate, the pressure decreases while the temperature in the sand continues to increase due to the exothermic reaction. After the initial rapid formation of hydrate, the growth rate of hydrate gradually decreases and the temperature will also decrease gradually after attaining a maximum value and tend to be stable at the temperature of air chamber after hydrate formation is finished, while the pressure also tends to be a constant value.

For the electrical resistivity, as shown in Figure 4d, at the initial stage that hydrate crystals start to form, there is a little decrease in resistivity, which varies from 1.17 Ω·m to 1.13 Ω·m. This phenomenon was also observed by Li et al.[17] The reason mainly lies on two aspects. First, it arises from the increase of ion concentration due to the consumption of water and methane gas at the early stage of nucleation of tiny hydrate crystals. Second, the speed of ion migration in the aqueous solution increases with the increase of temperature caused by gas injection of higher temperature and exothermic effect of hydrate formation. In comparison, the latter aspect plays a predominant role before aggregation of hydrate nuclei. However, the decrease of resistivity affected by the exothermic effect was not obvious when at low initial brine saturation, as shown in Figure 4a and b. Subsequently, the massive tiny hydrate nuclei keeps growing and then aggregating. Some intergranular throats become blocked by the formed hydrate, which results in poor connectivity of the aqueous solution. In this stage, the electrical resistivity would increase until it achieves a constant value after the pore throats are totally blocked by hydrate. The reason that the resistivity increases quickly during hydrate formation process can be explained by the blocking mechanism of both gas and hydrate in pores, as shown in Figure 5.[18] Before hydrate formation, as shown in Figure 5a, the random packing grain particles were partially saturated by brine. A thin adsorbed brine layer coats the sediment grains and connects in the pore space so that ions in pore fluid could migrate freely in the pores. When hydrate formation starts, as shown in Figure 5b, the formed tiny hydrate crystals appear and exist in the brine water, but are not large

Table 2. Resistivity of Methane Hydrate-Bearing Sediment for Five Groups of Samples at Different Initial Brine Saturation under Corresponding Temperature and Pressure

	before hydrate formation				after the end of hydrate formation				
run	S_w (%)[a]	P, MPa	T (K)	ρ_t (Ω·m)[b]	P (MPa)	T (K)	ρ_t (Ω·m)	S_h (%)[c]	x (%)[d]
1	12	7.22	277.5	11.29	6.44	277.9	39.28	12.4	82.8
2	20	7.89	277.1	3.76	6.86	277.8	18.43	15.8	63.7
3	30	7.88	276.2	1.83	6.78	276.8	11.71	24.3	67.2
4	40	8.05	275.8	1.17	5.83	276.2	3.14	33.0	67.7
5	50	8.13	277.3	0.88	5.19	275.8	2.08	40.3	64.0

[a] S_w—brine saturation. [b] ρ_t—resistivity. [c] S_h—hydrate saturation. [d] x—conversion ratio of water to hydrate.

dx.doi.org/10.1021/ef301257z | Energy Fuels 2012, 26, 6210−6217

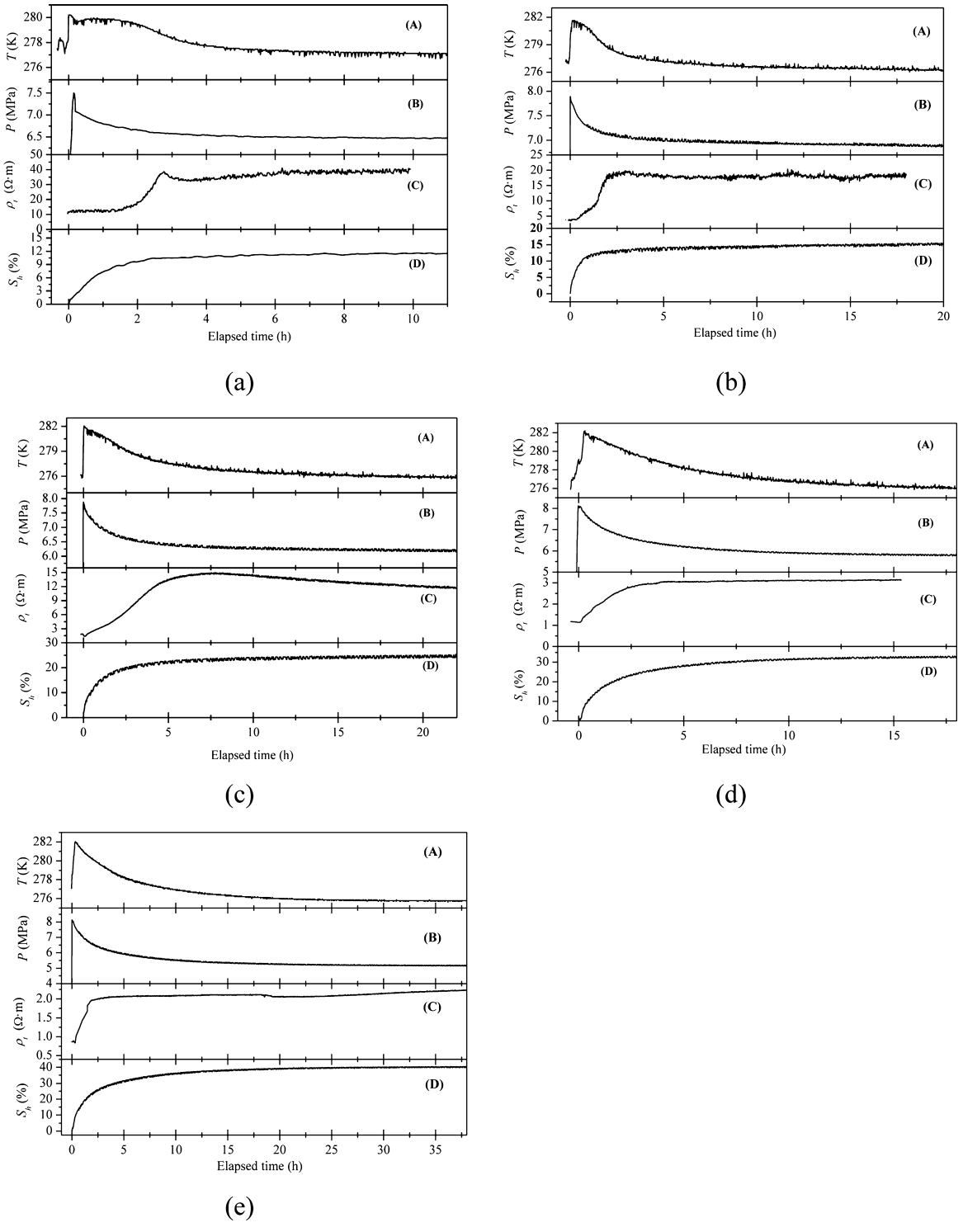

Figure 4. Variation of the temperature, pressure, resistivity, and hydrate saturation with the elapsed time for 60−80 meshes sandy sediment during methane hydrate formation under different initial brine saturation: (a) S_w = 12%; (b) S_w = 20%; (c) S_w = 30%; (d) S_w = 40%; (e) S_w = 50%.

enough to block the migration of ions. Meanwhile, the temperature will increase by 2 to 3 K due to the exothermic reaction, and then, the measured resistivity values will decrease slightly, as shown in Figure 4. With more and more hydrate crystals continuing forming, hydrate starts to accumulate and cement sediment grains, subsequently blocks the pores, as shown in Figure 5c, resulting in the measured resistivity increases with the elapsed time. After the pores in the sediment that ions could pass through were completely blocked, the electrical resistivity would not increase, even if the fraction of hydrate continues increasing a little.

For hydrate saturation, as shown in Figure 4d, it increases rapidly at the beginning stage of hydrate formation and gradually attains a maximum of 33.0%. According to the variation lines of resistivity and hydrate saturation in Figure 4d, the electrical resistivity achieves a maximum value of 3.14 Ω·m in 5 h and tends to be constant thereafter, while the hydrate saturation increases to be 27.6% at 5 h but it still continues to

dx.doi.org/10.1021/ef301257z | Energy Fuels 2012, 26, 6210−6217

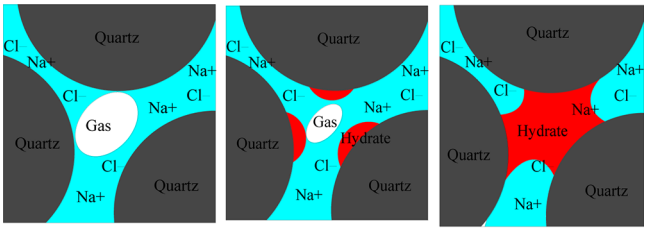

Figure 5. Schematic diagram of hydrate blocking mechanism during hydrate formation: (a) before hydrate formation; (b) hydrate formation start; (c) after the end of hydrate formation.

increase slowly with the elapse time and to be 33.0% at end. There exists an exponential relationship between hydrate saturation and resistivity, which indicates that hydrate content is not the only influence factor of the resistivity of hydrate-bearing sediment. The measurement of temperature and pressure in Figure 4d could mirror the result of resistivity.

There is a noticeable decrease of the electrical resistivity after 8.2 h for the experimental run with an initial brine saturation of 30%, as shown in Figure 4c. Its behavior shows a different trend compared with that of the other four experimental runs, in which the resistivity tends to be constant at the maximum value when pore channels are blocked. This slight decrease may be related to the initial mixing degree of brine with sediment and the migration of brine solution within the pore space of the sediment over the hydrate formation process.

The final stable value of electrical resistivity after the end of hydrate formation at different initial brine volumes were shown in Table 2. It has a wide range, which is 39.28 Ω·m, 18.43 Ω·m, 11.71 Ω·m, 3.14 Ω·m, and 2.08 Ω·m for the initial brine saturation of 12%, 20%, 30%, 40%, and 50%, respectively, corresponding to the final hydrate saturation of 12.4%, 15.8%, 24.3%, 33.0%, and 40.3%. It suggests that resistivity is larger even the hydrate concentration is lower. It is more affected by the free methane gas and brine saturation in the pore space of the sediment. Free gas is most associated with hydrate deposits.[30] The technology of Bottom Simulating Reflection (BSR) on seismic records is related to the effects of free gas on hydrate locations.[31] During the hydrate formation, the presence of free gas in the pores of the sediment will influence on the measured results of electrical resistivity. On the other hand, if the fraction of free gas in pore space of the sediment is higher, the initial brine saturation would be lower before hydrate formation. Therefore, the number of ion in the residual pore water is less and the resistivity of formed hydrate-bearing sample would be large. So, the measured results of electrical resistivity increase with the decrease of initial brine saturation in pore space.

There exist some differences among literature data of resistivity for hydrate-bearing sediment due to the difference of experimental conditions. For hydrate-bearing samples formed from 2 wt % brine-saturated sediment and methane gas, the resistivity varies from 11 to 13 Ω·m after hydrate formation is completed.[17] For a large sandpack with the mass concentration of brine is 3.5%, the electrical resistivity varies from 1.24 to 3.82 Ω·m when hydrate saturation increased from 0 to 67.0% of the pore space at different gas hydrate saturations.[18] For an originally fully water saturated glass bead sample, the electrical resistivity is 5.1 Ω·m; it increases to 265 Ω·m at about 95% hydrate saturation, whereas the water resistivity decreases from 1.39 Ω·m to 1.08 Ω·m.[19] These results suggest that the difference of resistivity for hydrate sample is due to the brine concentration and pore-filling materials.

3.3. Parameters Fitting in Archie Formulation. The Archie equation[32] was first used as a qualitative way to evaluate the amount of oil and gas reservoirs in the exploitation. Pearson et al.[33] suggested the use of Archie's law to determine the amount of hydrate in the sediment from in situ measurements of electrical properties. According to Archie equation, there exist two equations. The first equation is for fully brine-saturated sediment with a resistivity ρ_0,[8,15,20,32]

$$\rho_0 = F_0\rho_w = \frac{a}{\phi^m}\rho_w; \qquad F_0 = \frac{a}{\phi^m} \tag{7}$$

where ρ_w is the resistivity of the brine in the pore space of the sediment; F_0 is the formation resistivity factor of the fully brine-saturated sediment; ϕ is the porosity of the sediment; and a is a coefficient of additional skeleton conductivity, which is equal to 1 when the sediment frame is nonconducting.

The second Archie equation is for hydrate-bearing sediment with a resistivity ρ_t when the pores of the sediment are completely saturated with brine and hydrate. The formation resistivity index can be written as[19]

$$I = \frac{\rho_t}{\rho_0} = \frac{b}{S_w^n} \tag{8}$$

where I is resistivity index of hydrate-bearing sediment; n is a saturation exponent; and b is a coefficient describing whether hydrates disperse homogenously in the pore space of hydrate-bearing sediment, which is equal to 1 when the hydrate sample is formed with an uniform distribution.

By combining eqs 7 and 8, we obtain

$$\frac{\rho_t}{\rho_w} = \frac{ab}{S_w^n\phi^m} \tag{9}$$

There are four parameters a, b, m, and n in eq 9, indicating that it is extremely difficult to obtain hydrate saturation in the sediment by using this equation. If assuming that free gas does not exist in the sediment, only hydrate and liquid water exist in the pore space, that is, $S_h + S_w = 1$. The porosity would decrease with the increase of hydrate saturation in the pore space of the sandy sediment

$$\phi = \phi_0(1 - S_h) \tag{10}$$

where constant ϕ_0 is the initial porosity of the sediment packs, as defined above. Then eq 9 can be changed as follows:

$$\frac{\rho_t}{\rho_w} = \frac{ab}{(1 - S_h)^{m+n}\phi_0^m} \tag{11}$$

Using the log function on both sides of eq 11, it becomes

$$\ln\left(\frac{\rho_t}{\rho_w}\right) = -(n + m)\ln(1 - S_h) - m\ln\phi_0 + \ln(ab) \tag{12}$$

In this work, parameters a and b are equal to 1, so eq 12 can be simplified as

$$\ln\left(\frac{\rho_t}{\rho_w}\right) = -(n + m)\ln(1 - S_h) - m\ln\phi_0 \tag{13}$$

dx.doi.org/10.1021/ef301257z | Energy Fuels 2012, 26, 6210−6217

It definitely shows that there exists linear relationship between (ρ_t/ρ_w) and $1 - S_h$ on log−log coordinates. The parameters m and n can be obtained through experimental data.

The formed gas hydrate sample was a mixture of sandy sediment, hydrate, and free methane gas. The free pore space of the sediment was filled with methane gas and the remaining brine. It is known that Archie's Law is well established only for rock saturations created by capillary drainage. For the hydrate-bearing sediment, the pore space must be fully saturated with brine. In contrast, to obtain the parameters m and n in Archie equation and apply the Archie law to hydrate-bearing sediment, in this work, we first form partially hydrate-saturated samples. To eliminate the influence factor of free gas in the pores, after the partially hydrate-saturated sample for a given initial brine concentration was formed, the brine (with a concentration of 3.35 wt %) saturated with methane gas was injected into the high pressure reactor through a pipeline fixed on the top lid of the cell in Figure 2. The temperature of the brine solution was at 276.2 K during the injection process. The whole process was conducted within the hydrate stability zone and methane hydrate would not dissociate. After the space of the free gas was occupied by brine, the electrical resistivity was subsequently measured, and the results are listed in Table 3. Parameters m and n in eq 13 could be calculated with the final measured resistivity at different hydrate saturations. It obviously shows that resistivity increases with the increase of hydrate volume from 12.4% to 40.3% when the pore space is completely filled with brine solution after brine injection. The variation of (ρ_t/ρ_w) versus $1 - S_h$ was plotted in Figure 6 in a double logarithmic coordinate axis. It clearly shows that there is a linear relationship between $\ln(\rho_t/\rho_w)$ and $\ln(1 - S_h)$. According to the intercept and slope value of the fitting line, parameters m and n were determined as 0.1677 and 1.6019, respectively, while the initial porosity of the sandy sediment ϕ_0 is 0.416. The empirical saturation exponent n is controlled by the lithology, hydrate distribution (uniform or not), and the intergranular connectivity of the sandy packs.[20,33] Experimental investigation on the saturation exponent n of unconsolidated sediments was 1.9386,[33] which is a little higher than that fitted in this work. This probably lies in the different experimental conditions, such as the internal pore structure, and the distribution of the hydrate in the sediment. The relationship between hydrate saturation in the pore space and total electrical resistivity of the hydrate-saturated sediment could then be described as

$$\frac{\rho_t}{\rho_w} = \frac{1}{(1 - S_h)^{1.7696}\phi_0^{0.1677}} \quad (14)$$

Figure 7 shows the relative electrical resistivity as a function of hydrate volume in the pore space of the sediment. It can be found that the calculated results fit in absolutely well with the experimental data for five experimental runs in this work. In other words, the fitted parameters of m and n in Archie formulation are obviously reasonable in calculating hydrate saturation in the sediment.

Table 3. Resistivity of Hydrate-Bearing Sediment before and after Brine Injection

	before brine injection			after brine injection			
run	S_h (%)	ρ_t (Ω·m)	$\ln(1 - S_h)$	ρ_w (Ω·m)	ρ_t (Ω·m)	ρ_t/ρ_w	$\ln(\rho_t/\rho_w)$
1	12.4	39.28	−0.13	0.33	0.45	1.38	0.32
2	15.8	18.43	−0.17	0.30	0.47	1.57	0.45
3	24.3	11.71	−0.28	0.25	0.50	2.01	0.70
4	33.0	3.14	−0.40	0.23	0.59	2.52	0.92
5	40.3	2.08	−0.52	0.22	0.61	2.72	1.00

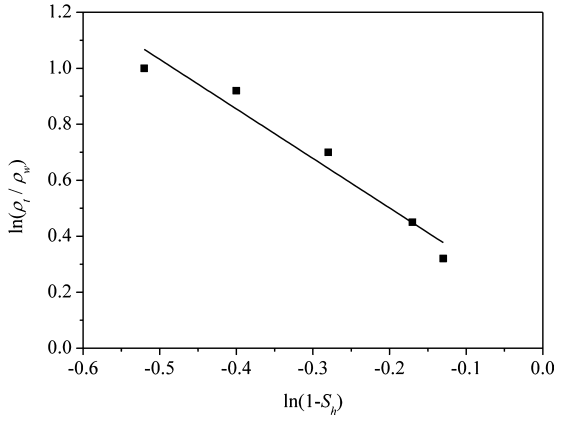

Figure 6. Plot of (ρ_t/ρ_w) as a function of $1 - S_h$ in double logarithmic coordinate axis.

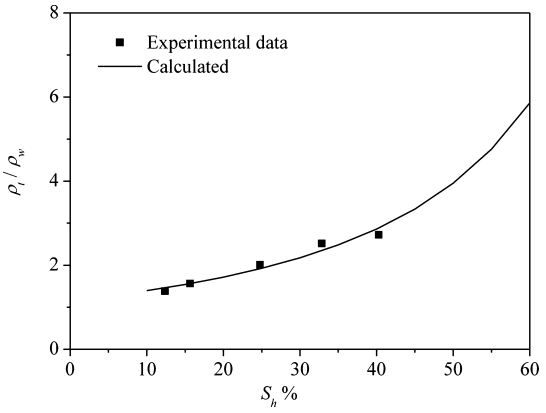

Figure 7. Comparison of resistivity of experimental data and calculated results for five experimental runs.

4. CONCLUSIONS

An experimental setup was built to study the evolvement of electrical properties during the hydrate formation process, where a two-electrode configuration was in situ used to measure the electrical resistivity of the hydrate-bearing sediment. The experimental results of five groups of methane hydrate samples formed with different initial brine saturation showed that the electrical resistivity of the mixtures depends on the fluid-filled porosity, hydrate saturation in the pores, temperature, ionic concentration of the pore fluid, and other factors, such as lithology, hydrate distribution in the pore space of the sediment. The formation of methane hydrate within the pores of sand packs substantially alters the electrical properties of fluid-saturated sediment, expressed in the form of electrical resistivity. For hydrate samples at different initial brine saturations, the values of electrical resistivity are larger even though hydrate saturation is lower if free methane gas exists in sediment pores. Based on the experimental results of hydrate concentration and resistivity measured after brine injection process, the empirical parameters of m and n in Archie formulation were fitted, which would be helpful for evaluating

dx.doi.org/10.1021/ef301257z | Energy Fuels 2012, 26, 6210−6217

hydrate saturation in hydrate-bearing sediment by electrical resistivity based on Archie formulation.

AUTHOR INFORMATION

Corresponding Author

*Fax: +86 10 89733156. E-mail: cysun@cup.edu.cn (C.Y.S.); gjchen@cup.edu.cn (G.J.C.).

Notes

The authors declare no competing financial interest.

ACKNOWLEDGMENTS

The financial support received from the National 973 Project of China (No. 2009CB219504), the National Natural Science Foundation of China (Nos. 20925623, U1162205, 21076225), and Science Foundation of China University of Petroleum, Beijing (LLYJ-2011-63) is gratefully acknowledged.

REFERENCES

(1) Sloan, E. D. Fundamental principles and applications of natural gas hydrates. *Nature* **2003**, *426*, 353−359.

(2) Johnson, A. H. Global resource potential of gas hydrate − a new calculation. *Fire in the Ice, Methane Hydrate Newsletter* **2011**, *11*(2), 1−4. Available online: http://seca.doe.gov/technologies/oil-gas/publications/Hydrates/Newsletter/MHNews-2011-12.pdf

(3) Weitemeyer, K. A.; Constable, S. C.; Key, K. W.; Behrens, J. P. First results from a marine controlled-source electromagnetic survey to detect gas hydrates offshore Oregon. *Geophys. Res. Lett.* **2006**, *33*, L03304.

(4) Collett, T. S.; Lee, M. W.; Zyrianova, M. V.; Mrozewski, S.; Guerin, G.; Cook, A.; Goldberg, D. Gulf of Mexico gas hydrate joint industry project. Leg II. Logging-while-drilling data acquisition and analysis. *Mar. Pet. Geol.* **2012**, *34*, 41−61.

(5) Collett, T. S.; Lewis, R.; Winters, W. J.; Lee, M. W.; Rose, K. K.; Boswell, R. M. Downhole well log and core montages from the Mount Elbert gas hydrate stratigraphic test well, Alaska North Slope. *Mar. Pet. Geol.* **2011**, *28*, 561−577.

(6) Cook, A. E.; Anderson, B. I.; Rasmus, J.; Sun, K. L.; Li, Q. M.; Collett, T. S.; Goldberg, D. S. Electrical anisotropy of gas hydrate-bearing sand reservoirs in the Gulf of Mexico. *Mar. Pet. Geol.* **2012**, *34*, 72−84.

(7) Cranganu, C.; Bautu, E. Using Gene Expression Programming to estimate sonic log distributions based on the natural gamma ray and deep resistivity logs: A case study from the Anadarko Basin, Oklahoma. *J. Pet. Sci. Eng.* **2010**, *70*, 243−255.

(8) Kamel, M. H.; Mabrouk, W. M. An equation for estimating water saturation in clean formations utilizing resistivity and sonic logs: theory and application. *J. Pet. Sci. Eng.* **2002**, *36*, 159−168.

(9) Salem, H. S.; Chilingarian, G. V. Determination of specific surface area and mean grain size from well-log data and their influence on the physical behavior of offshore reservoirs. *J. Pet. Sci. Eng.* **1999**, *22*, 241−252.

(10) Shankar, U.; Riedel, M. Gas hydrate saturation in the Krishna−Godavari basin from P-wave velocity and electrical resistivity logs. *Mar. Pet. Geol.* **2011**, *28*, 1768−1778.

(11) Sun, Y.; Goldberg, D.; Collett, T.; Hunter, R. High-resolution well-log derived dielectric properties of gas-hydrate-bearing sediments, Mount Elbert gas hydrate stratigraphic test well, Alaska North Slope. *Mar. Pet. Geol.* **2011**, *28*, 450−459.

(12) Du Frane, W. L.; Stern, L. A.; Weitemeyer, K. A.; Constable, S.; Pinkston, J. C.; Roberts, J. J. Electrical properties of polycrystalline methane hydrate. *Geophys. Res. Lett.* **2011**, *38*, L09313, doi:10.1029/2011GL047243.

(13) Buffett, B. A.; Zatsepina, O. Y. Formation of gas hydrate from dissolved gas in natural porous media. *Mar. Geol.* **2000**, *164*, 69−77.

(14) Zatsepina, O. Y.; Buffett, B. A. Experimental study of the stability of CO_2-hydrate in a porous medium. *Fluid Phase Equilib.* **2001**, *192*, 85−102.

(15) Pearson, C.; Murphy, J.; Hermes, R. Acoustic and resistivity measurements on rock samples containing tetrahydrofuran hydrates: laboratory analogues to natural gas hydrate deposits. *J. Geophys. Res.* **1986**, *91* (B14), 14132−14138.

(16) Lee, J. Y.; Santamarina, J. C.; Ruppel, C. Parametric study of the physical properties of hydrate-bearing sand, silt, and clay sediments: 1. Electromagnetic properties. *J. Geophys. Res.* **2010**, *115* (B11), B11104.

(17) Li, S. X.; Xia, X. R.; Xuan, J.; Liu, Y. P.; Li, Q. P. Resistivity in formation and decomposition of natural gas hydrate in porous medium. *Chin. J. Chem. Eng.* **2010**, *18*, 39−42.

(18) Ren, S. R.; Liu, Y. J.; Liu, Y. X.; Zhang, W. D. Acoustic velocity and electrical resistance of hydrate bearing sediments. *J. Pet. Sci. Eng.* **2010**, *70*, 52−56.

(19) Spangenberg, E. Modeling of the influence of gas hydrate content on the electrical properties of porous sediments. *J. Geophys. Res.* **2001**, *106* (B4), 6535−6548.

(20) Spangenberg, E.; Kulenkampff, J. Influence of methane hydrate content on electrical sediment properties. *Geophys. Res. Lett.* **2006**, *33*, L24315.

(21) Hovland, M.; Gallagher, J.; Clennell, M.; Lekvam, K. Gas hydrate and free gas volumes in marine sediments: Example from the Niger Delta front. *Mar. Pet. Geol.* **1997**, *14*, 245−255.

(22) Li, F. G.; Sun, C. Y.; Zhang, Q.; Liu, X. X.; Guo, X. Q.; Chen, G. J. Laboratory measurements of the effects of methane/tetrahydrofuran concentration and grain size on the P-wave velocity of hydrate-bearing sand. *Energy Fuels* **2011**, *25*, 2076−2082.

(23) Yang, X.; Sun, C. Y.; Yuan, Q.; Ma, P. C.; Chen, G. J. Experimental study on gas production from methane hydrate-bearing sand by hot-water cyclic injection. *Energy Fuels* **2010**, *24*, 5912−5920.

(24) Yuan, Q.; Sun, C. Y.; Yang, X.; Ma, P. C.; Ma, Z. W.; Li, Q. P.; Chen, G. J. Gas production from methane hydrate bearing sands by ethylene glycol injection using a three-dimensional reactor. *Energy Fuels* **2011**, *25*, 3108−3115.

(25) Chen, G. J.; Guo, T. M. A new approach to gas hydrate modelling. *Chem. Eng. J.* **1998**, *71*, 145−151.

(26) Zhang, Q.; Li, F. G.; Sun, C. Y.; Li, Q. P.; Wu, X. Y.; Liu, B.; Chen, G. J. Compressional wave velocity measurements through sandy sediments containing methane hydrate. *Am. Mineral.* **2011**, *96*, 1425−1432.

(27) Jung, J. W.; Espinoza, D. N.; Santamarina, J. C. Properties and phenomena relevant to CH_4−CO_2 replacement in hydrate-bearing sediments. *J. Geophys. Res.* **2010**, *115* (B10), B10102.

(28) Peng, D. Y.; Robinson, D. B. A new two-constant equation of state. *Ind. Eng. Chem. Fund.* **1976**, *15*, 59−64.

(29) Hyndman, R. D.; Yuan, T.; Moran, K. The concentration of deep sea gas hydrates from downhole electrical resistivity logs and laboratory data. *Earth Planet. Sci. Lett.* **1999**, *172*, 167−177.

(30) Suess, E.; Torres, M.; Bohrmann, G.; Collier, R.; Rickert, D.; Goldfinger, C.; Linke, P.; Heuser, A.; Sahling, H.; Heeschen, K.; Jung, C.; Nakamura, K.; Greinert, J.; Pfannkuche, O.; Trehu, A.; Klinkhammer, G.; Whiticar, M.; Eisenhauer, A.; Teichert, B.; Elver, M. Sea floor methane hydrates at Hydrate Ridge, Cascadia margin. In *Natural Gas Hydrates: Occurrence, Distribution, and Detection*; AGU: Washington, DC, 2001; pp 87−98.

(31) Kuustraa, V. A.; Hammershaimb, E. C. *Handbook of Gas Hydrate Properties and Occurrence*, DOE/MC/19239-1546; Lewin and Associates, Inc.: Washington, DC, 1983.

(32) Archie, G. E. The electrical resistivity log as an aid in determining some reservoir characteristics. *Trans. AIME* **1942**, *146* (99), 54−62.

(33) Pearson, C. F.; Halleck, P. M.; McGuire, P. L.; Hermes, R.; Mathews, M. Natural gas hydrate deposits: A review of in situ properties. *J. Phys. Chem.* **1983**, *87*, 4180−4185.